a.i. solutions®

Assessing Performance Characteristics of the SGP4-XP Propagation Algorithm

Written by: Dave Conkey & Mitchell Zielinski

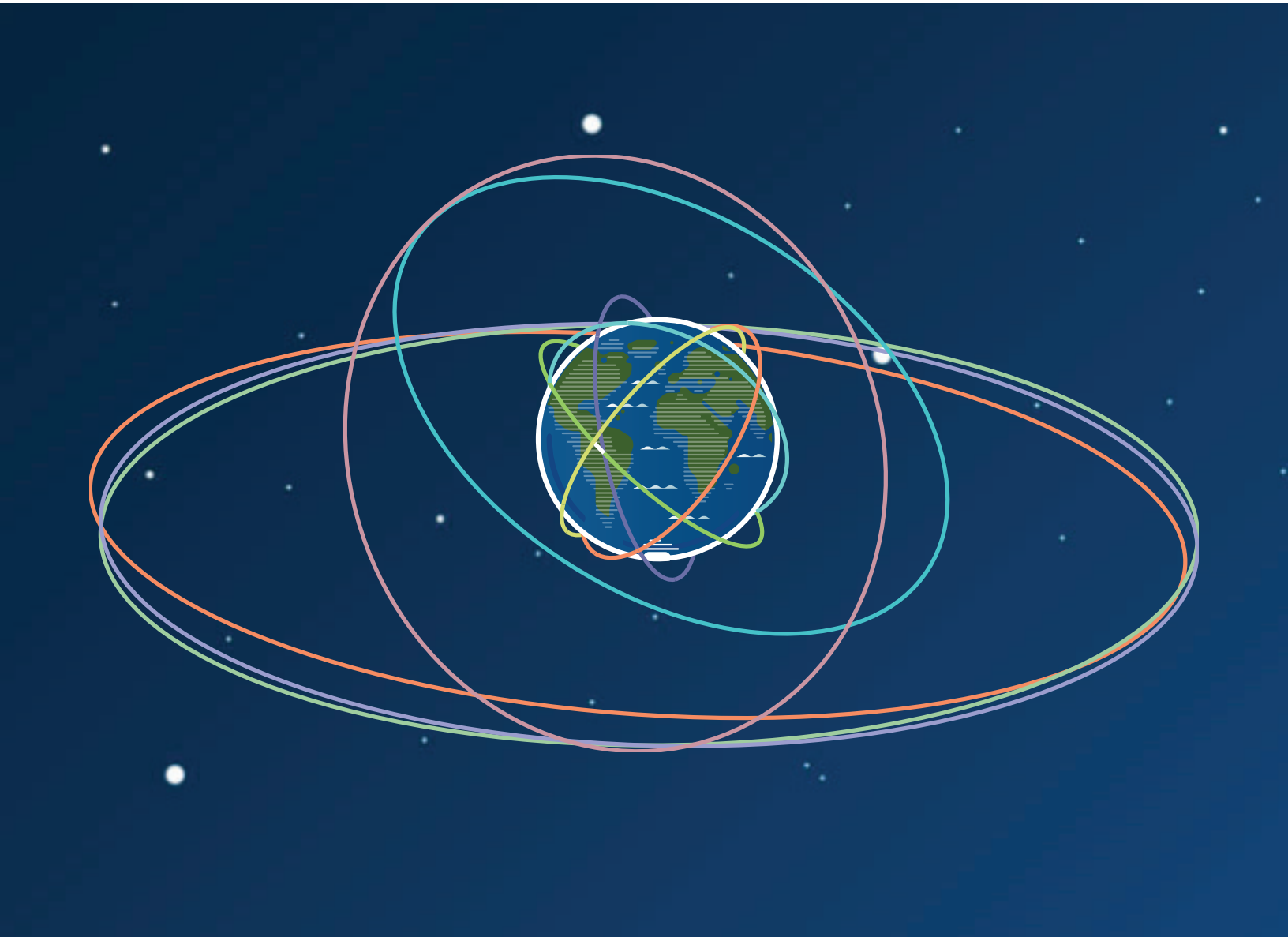

Assessing Performance Characteristics of the SGP4-XP Propagation Algorithm

Dave Conkey
a.i. solutions
Mitchell Zielinski
a.i. solutions

ABSTRACT

In 2020 the United States Space Force (USSF) released an implementation of the SGP4-XP propagator, an advanced version of the existing SGP4 propagator stated to deliver accuracy roughly equivalent to that of the USSF's Special Perturbations Ephemeris propagator (SPEPH) with runtimes only 50% to 100% longer than SGP4. This paper presents an analysis of the performance characteristics of the SGP4-XP propagation algorithm and considers new and existing practical applications where it can be used more effectively than SGP4. To perform this analysis two-line elements sets (TLE's) are generated from high-precision reference ephemerides for a selection of objects across different orbital regimes using the USSF implementations of both the SGP4 and SGP4-XP propagators. The fit accuracy of each set of TLE's is assessed by evaluating how well the propagation of the generated TLE's compare to the initial reference trajectory. Runtime performance is assessed by measuring the elapsed wall-clock time to propagate a TLE over the fit span.

The SGP4-XP algorithm was found to have significantly improved position accuracy compared to SGP4 for objects in medium and high Earth orbits. Position accuracy for objects in low-Earth orbit was comparable to that of SGP4, but velocity accuracy proved to be better which improves accuracy when propagating beyond the fit-span of the TLE generation process. The significance of the improved performance characteristics of the SGP4-XP are evaluated in the context of the impact that they have on an example contact analysis and conjunction assessment scenario.

1. BACKGROUND

The Simplified General Perturbations 4 (SGP4) model was developed in 1970 for the propagation of near-Earth satellite trajectories. This algorithm was made publicly available in 1980 with the publication of *Spacetrack Report No. 3* [1]. The report contained the equations for the algorithm as well as FORTRAN source code. Various updates have been made over the years since the first publication, but the underlying algorithm has remained basically the same. The algorithm is widely used for the propagation of Two-Line Element (TLE) sets [2]. Over the years there has been a proliferation of versions of the algorithm in the aerospace community in various programming languages, refactored in various ways, and updated at various intervals. Additionally, for most commonly used implementations, there is no mechanism to enforce or evaluate what version is being used and what updates have been applied. Ultimately, this has led to differences between the propagation used in the USSF's TLE generation process and the propagated trajectory of a TLE state using a non-official implementation of the SGP4. This was confirmed in 1990 when a copy of the current operational SGP4 code used to generate publicly-distributed TLEs was made available to the public. In 2006 Vallado et al. used the definitive set of SGP4 equations published in [3] to develop a non-proprietary implementation of SGP4 that replicated the behavior of the operational implementation.

To attempt to remedy this problem, the United Space Air Force (USAF, now the USSF) began releasing an official implementation of the SGP4 algorithm that is used in operations as part of the AstroStds software library [4]. Initially, this library was export controlled, but as of the release of version 8.x it is now available with access to the space-track.org website under the label of "non-restricted access".

In addition to the official implementation of the SGP4 algorithm, the AstroStds library contains the Special Perturbations Ephemeris propagator (SPEPH). The SPEPH is an implementation of a Runge-Kutta numerical integrator with high-fidelity force models. This propagator is the best-available trajectory propagation algorithm used by the USSF, but is still export controlled.

While TLE's and associated SGP4 propagation are widely used for many applications, traditionally the intent has been for it to provide fast and / or computationally efficient trajectory propagation in domains where significant error is acceptable. The classic example is for use at ground-sites performing antenna pointing with a wide field of view (FOV). The accuracy of TLE propagation using SGP4 is summarized in [5]. In-track error dominates, and can grow as large as 25 km after only a few days of propagation. Also, [6] found that the error has a significant bias, especially in the in-track direction, and the minimum error does not necessarily occur at the epoch defined in the TLE state.

As the use of TLE's and SGP4 propagation has become more ubiquitous, the requirements and problems in modern space mission operations have evolved. A few examples include tighter pointing requirements to support higher data transfer rates and the evolution of space-situational awareness (SSA) and space-domain awareness (SDA) priorities.

To address some of these issues, in December 2020 the USSF released an implementation of the SGP4-XP algorithm with version 8 of the SGP4 library as part of the AstroStds library. The SGP4-XP is a new algorithm designed for the propagation of TLEs featuring "extended perturbations". The release notes associated with this release [4] claim that SGP4-XP is "appropriate for applications that require SPEPH-level accuracy". The SGP4-XP algorithm continues to operate using the same basic set of information that is in the existing TLE format, meaning all users need to do to take advantage of the new algorithm is to upgrade to the new version of the SGP4 library.

The release notes associated with the SGP4-XP reference the following improvements:

- Improved lunar perturbation modeling
- New and more resonance modeling for different orbit regimes
- Solar radiation pressure (SRP) modeling for all orbit regimes
- The Geopotential model now includes the J5 zonal term
- The legacy WGS-72 terms are replaced with EGM-96 terms
- The static atmosphere model is replaced with the Jacchia-70 atmospheric density model

Additional details regarding how the values in the TLE are different for an SGP4-XP derived TLE can be found in the release notes for the AstroStds library [4]. One point to note is that SGP4-XP derived TLE's are signified by setting the "Ephemeris Type" field to a value of 4. This leads to the usage of the terms "type 4 ephemeris" or "type 4 TLE".

2. NOMENCLATURE

Throughout this paper the following terminology will be used:

- Algorithm versus Implementation: The term algorithm refers to the actual physical models and math associated with a given propagation model. The implementation is the library ("dll" on Windows and "so" on Linux) that is used by the software to perform the analysis. The SGP4 **algorithm** is documented in [1]. The SGP4 and SGP4-XP **implementations** are provided in .dll's / .so's provided by the USSF on the space-track.org website. The SGP4-XP algorithm isn't fully documented in the public domain at this time.
- SGP4 versus Classical SGP4 versus SGP4-XP: When not explicitly stated, usage of the term SGP4 applies to both the SGP4 and SGP4-XP algorithms. For example, the USSF provides the SGP4 library which provides implementations of both the **Classical SGP4** algorithm and the "Extended Perturbation" **SGP4-XP** algorithm. The **Classical SGP4** refers to the SGP4 algorithm that was first released in 1980. The **SGP4-XP** refers to the new enhanced algorithm released in 2020 as part of version 8 of the AstroStds library.
- SGP4 State: The set of mean Keplerian elements used as inputs to the classical SGP4 algorithm, plus state epoch and B^*. In this context B^* acts as either a drag term or an SRP term depending on the orbital period.
- SGP4-XP State: Same as the SGP4 state, but with a dedicated SRP term called AGOM (Area times Gamma over Mass) to support modeling drag and SRP simultaneously.

- Special Perturbations (SP) State: A state derived using a high-fidelity force model and numeric integrator. An SP State may come from the SPEPH propagator, or another high-accuracy numeric propagator such as FreeFlyer's RK89.
- General Perturbations (GP) State: A state derived from low-fidelity an analytic or semi-analytic propagator such as the SGP4.
- TLE: Two-Line Element, the basic format for serializing elements of the SGP4 / SGP4-XP state

3. TLE GENERATION METHODOLOGY

The general methodology used for generating a TLE is to solve for a single Keplerian state that when propagated with an SGP4 algorithm minimizes the error between the propagated state and some other set of data that provides information as to the nature of the orbit, i.e. observations from a tracking station. In practice the algorithm used to perform this optimization is a standard batch-least-sqaures (BLS). So, in that way the problem takes the form of any other sort of orbit determination (OD). The inputs are then simply an a priori state, covariance, a set of observations to process, and various tuning parameters.

This approach can be used with any sort of observation model that provides information about the orbit. This includes observations like ground-based or space-based angles (azimuth and elevation), range, range-rate / doppler, GPS / GNSS measurements, etc. Typically these types of observations are used in the context of propagating an initial state with a high-fidelity numeric integrator and force model to get a "Special Perturbations" (SP) state. However, some problems can be solved more efficiently using a coarse propagation model like that provided by the SGP4 algorithm. Examples of problems like these include poorly tracked states and / or observations that are particularly noisy.

Often in operations, particularly for missions that generate their own TLE's, the SP state is determined first, and then a General Perturbations (GP) state is derived from that using an implementation of the SGP4 algorithm. In this approach, the SP state is propagated over a specified "fit-span" and states from that propagation are sampled at some interval to form "observations". This allows for a calculation of mean Keplerian state that best matches the provided trajectory as propagated with an SGP4 propagator. FreeFlyer, a commercial off-the-shelf software (COTS) astrodynamics tool, includes features for performing this process, and was used in the analysis for this paper.

The key orbital parameters associated with a TLE are defined on the celestrak.org website [7]. These are essentially the standard Keplerian element set with mean motion taking the place of semi-major axis and the addition of a drag term (B^*) and / or AGOM. However, the classical Keplerian elements are not well suited for an optimization process given the indeterminate behavior of the Euler angles that define the orbit geometry. For this reason, the FreeFlyer estimation process uses a modified equinoctial formulation. This equinoctial formulation uses vectors scaled by eccentricity and inclination in place of the angles of the classical Keplerian set. The definition of the equinoctial system used by FreeFlyer in the estimation process is defined in [8].

Typically, when an SGP4 propagator is used to fit a high-fidelity SP trajectory, the a priori for the fit is provided as an instantaneous Cartesian state vector from the SP ephemeris. In FreeFlyer this state is then converted to an initial guess of a mean Keplerian state, then converted to an equinoctial state using the formulation noted above. Once the fit is complete, the estimated mean equinoctial state is converted back to a mean Keplerian state, and those terms are serialized into the TLE format.

To assess the quality of the generated TLE's, the TLE is deserialized and the mean state is propagated to each vector of the SP ephemeris using an SGP4 propagator. Metrics such as alongtrack, crosstrack, radial separation, and overall range between the states in the SP ephemeris and the SGP4 propagated states are evaluated.

4. ANALYSIS APPROACH

At the time of this writing the USSF isn't providing SGP4-XP TLE's in the public domain. So this paper outlines an approach to generate and evaluate SGP4-XP TLE's based upon high-fidelity numerical integration. This likely mirrors how the USSF will generate them using their SPEPH propagator. Since access to the SPEPH propagator is not available in the public domain, the FreeFlyer RK89 numeric integrator will be used for this analysis.

In order to justify this approach, first the FreeFlyer numerical integration is validated against publicly available high-precision Satellite Laser Ranging (SLR) ephemerides. This provides missions in the LEO and MEO orbit regimes. Unfortunately, that doesn't provide any in the GEO regime, which is a particular area of interest. To fill that void, four Intelsat missions located at different longitude crossings are also included.

Table 1 summarizes the orbital elements of the selected missions; and Figure 1 shows a notional representation of each mission's orbit.

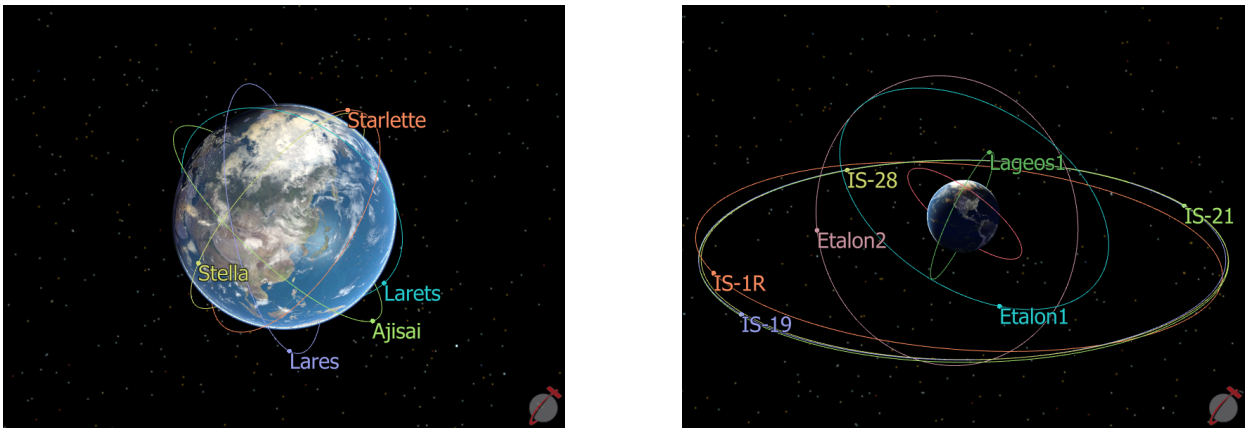

(a) Selected LEO Missions

(b) Selected MEO and GEO Missions

Fig. 1: Selected Missions

Table 1: Orbital Elements of Selected Missions

Mission	SMA (km)	Eccentricity	Inclination (deg)	Period (min)	Perigee (km)	Apogee (km)
Larets	7051	1.880e-03	98.13	98.21	7037.92	7064.43
Stella	7172	2.378e-03	98.91	100.76	7155.79	7189.90
Starlette	7340	2.103e-02	49.92	104.31	7185.80	7494.50
Lares	7813	1.096e-03	69.38	114.55	7804.61	7821.73
Ajisai	7861	1.513e-03	49.87	115.63	7850.10	7873.89
Lageos2	12163	1.319e-02	52.78	222.51	12003.11	12323.93
Lageos1	12265	4.304e-03	109.94	225.32	12213.00	12318.58
Etalon2	25501	1.662e-03	65.52	675.47	25459.00	25543.76
Etalon1	25501	2.266e-03	64.43	675.46	25443.36	25558.93
IS-28	41925	5.723e-03	0.16	1423.91	41685.97	42165.84
IS-1R	41926	5.651e-03	4.72	1423.95	41689.75	42163.65
IS-19	41926	5.384e-03	0.16	1423.95	41700.94	42152.37
IS-21	41925	5.807e-03	0.15	1423.88	41681.71	42168.66

Once the validity of the FreeFlyer numeric integrator is demonstrated, the classical SGP4 algorithm is used to generate TLE's. These TLE's are generated using both the SLR / Intelsat ephemerides and ephemerides generated using FreeFlyer integration as reference trajectories. The propagation of each set of SGP4 TLE's are compared against each other. This demonstrates the basic ability to perform SGP4 state estimation using FreeFlyer with different data sources.

After demonstrating the pipeline above works well, the next step is to use the SGP4-XP as the propagation algorithm when estimating the mean SGP4 state. This demonstrates the performance of the SGP4-XP algorithm as compared to the classical SGP4 algorithm.

The steps above lay the groundwork for future analysis by demonstrating the following capabilities:

- The ability of the FreeFlyer numerical integration to act sufficiently as a proxy for the SPEPH propagator
- The ability of FreeFlyer to generate classical SGP4 mean elements sets for TLE generation
- The ability of FreeFlyer to generate SGP4-XP based mean elements sets for TLE generation

Details and results from each of these sections are provided below. This establishes the validity of using the FreeFlyer numerical integration engine to simulate different scenarios to assess the discriminating capabilities of the SGP4-XP algorithm relative to the classical SGP4 algorithm.

5. RESULTS

5.1 Numerical Integration Validation

The first step in the analysis as described above is to demonstrate that the FreeFlyer numerical integration engine is a valid proxy for the SPEPH propagator used by the USSF. This is done using the FreeFlyer Runge-Kutta 8/9 (RK89) numeric integrator with the following force model:

- Earth Spherical Harmonic Gravity Field with EGM 96 coefficients for 30x30 Field
- 1976 / 1980 Earth Orientation model of nutation and precession
- Sun Point mass
- Moon Point mass
- JPL DE430 Solar System Ephemeris
- Jacchia-Roberts Atmospheric Drag Model
- Spherical SRP Model

The missions outlined in Table 1 above provide 5 LEO missions, 4 MEO missions, and 4 GEO missions to perform this assessment. It is worth noting that all data and libraries used to perform this analysis are in the public domain.

Two challenges present themselves with this approach. To properly model trajectories in the LEO regime, the physical characteristics of the spacecraft that drive the drag acceleration (ie. drag area and coefficient of drag (C_D)) need to be modeled. Similarly, for the MEO and GEO missions the physical characteristics driving the SRP acceleration (i.e. SRP area and coefficient of reflectivity (C_R)) need to be modeled. Additionally, the Intelsat missions only provide a position history and not velocity. To address these challenges, the missing information; specifically C_D and / or C_R for the SLR-based missions, and C_R and velocity for the Intelsat missions, is solved for in an orbit determination (OD) process. After solving for optimal values for the missing data and re-propagating the trajectories, the range between the propagated state and the reference ephemerides is evaluated. The results of this process are shown in Table 2:

Table 2: Trajectory Optimization Results

Mission	**Mean Range (m)**	**Max Range(m)**
Larets	21.6	92.2
Stella	12.6	48.1
Starlette	10.0	36.3
Lares	4.0	11.1
Ajisai	10.3	37.1
Lageos2	2.4	7.4
Lageos1	2.9	7.7
Etalon2	3.6	9.5
Etalon1	3.2	7.2
IS-28	618.8	1595.3
IS-1R	602.8	1465.0
IS-19	551.3	1367.4
IS-21	535.8	1335.4

As can be seen, the fit of the FreeFlyer propagation to the reference ephemerides for the SLR-based missions is very good. The additional challenge of solving for velocity for the Intelsat missions yields greater discrepancies between the Intelsat provided positional states and the FreeFlyer propagation fitted to those positions. It is also worth noting that at the large distances of GEO orbits, a larger absolute discrepancy is still a relatively small percentage of the overall state. However, to give this a bit more treatment, a characterization of the dynamics affecting the orbit from the Intelsat ephemeris and the FreeFlyer trajectory fit is examined.

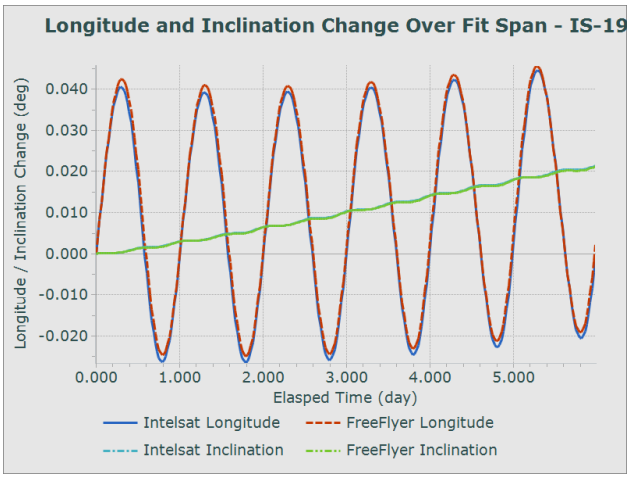

(a) IS-19 Longitude / Inclination Change

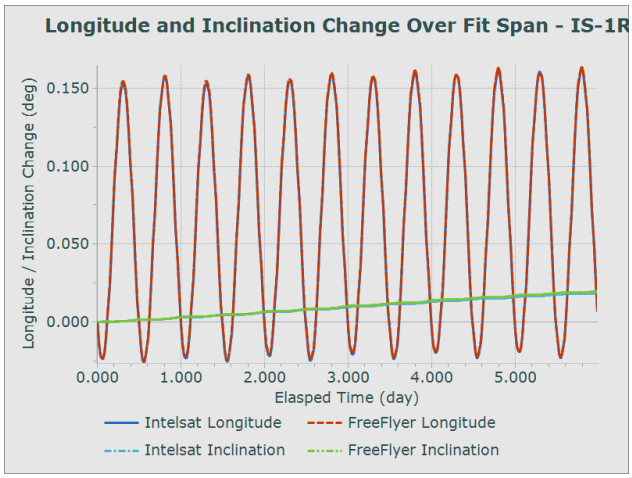

(b) IS-1R Longitude / Inclination Change

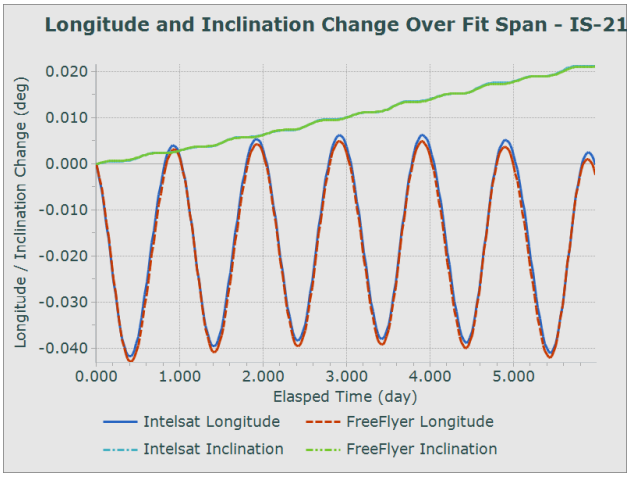

(c) IS-21 Longitude / Inclination Change

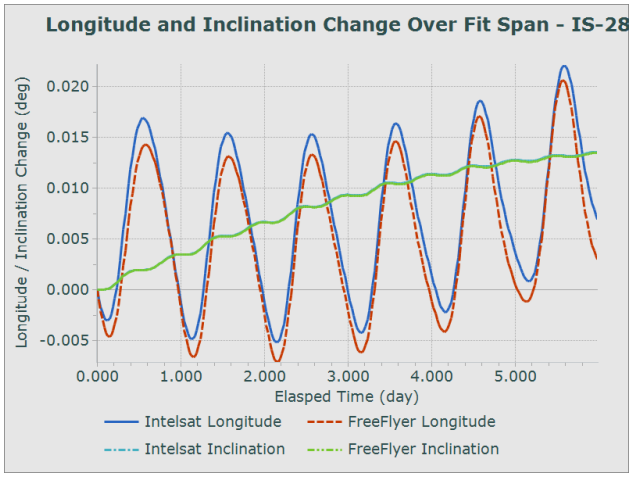

(d) IS-28 Longitude / Inclination Change

Fig. 2: GEO Missions Longitude / Inclination Trends

The plots in Figure 2 show the change in the longitude from the initial longitude at the start of the propagation span as the red and blue lines. The green and teal lines show the change in inclination from the initial inclination at the start of propagation span (in this case, they nearly overlap). These plots show that even though there is some positional discrepancies between the IntelSat ephemerides and the FreeFlyer integrated trajectories, the orbits exhibit consistent behaviors in their respective dynamical environments.

The results outlined above justify the use of the FreeFlyer RK89 as a suitable proxy for the SPEPH propagator. Henceforth, for the sake of simplicity and consistency, ephemerides generated via FreeFlyer integration will be used to evaluate the SGP4 / SGP4-XP fits.

5.2 General SGP4 Estimation Approach

The general approach for estimating SGP4 states and generating TLE's is really no different from any other trajectory fit process done in orbit determination, and follows the methodology discussed in Section 2. A set of "observations" are generated, an a priori state is determined, and the observations are processed as a set to minimize the residual between the propagated a priori state and the observations. This process is repeated until some convergence tolerance is satisfied.

The unique aspect in this context is that the propagation is done via the SGP4 algorithm, and the observations are Cartesian states pulled from the vectors of a reference ephemeris.

As with any trajectory fit process, there are still various tuning parameters to consider. SGP4 state estimation is

somewhat more limited given the crudeness of the model and only one term, B^*, to account for dynamical mismodeling (Note that the SGP4-XP also provides the ability to solve for AGOM along with B^*). Probably the most significant tuning parameter for SGP4 state estimation is fit-span, or the span of time over which the trajectory is sampled and optimized. This can be a delicate balance, as it is important to get enough data to sufficiently sample the dynamics of the orbit, but the SGP4 algorithm breaks down over long propagation times. There are general conventions used, and those are roughly followed here.

The SLR-based LEO missions provide reference ephemerides in approximately 4 day spans, which makes for a good choice to use for the fit-span given the volatile dynamics in that regime.

The MEO SLR-based missions provide ephemerides in approximately 7 day spans. For the GEO cases, the Intelsat-provided ephemerides span approximately 9 days. For these missions, a 6-day fit-span will be used. It understood that this is the typical default used operationally by the USSF as it sufficiently captures the dynamics of these relatively low dynamical environments, without surpassing the span in which the SGP4 algorithm is able to maintain a consistent accuracy.

5.3 Classical SGP4 TLE Generation

The results from the classical SGP4 TLE fit process are presented in Table 3.

Table 3: Classical SGP4 Fit Performance

Mission	Mean Range (km)	Max Range (km)
Larets	0.552	1.277
Stella	0.528	1.155
Starlette	0.368	0.883
Lares	0.385	1.163
Ajisai	0.283	0.680
Lageos2	0.188	0.457
Lageos1	0.125	0.280
Etalon2	0.283	0.725
Etalon1	0.244	0.696
IS-28	1.532	3.512
IS-1R	0.905	1.455
IS-19	7.440	15.144
IS-21	7.539	13.359

The main takeaway from this data is to ensure that for all cases the fit quality is what would be expected for a given orbit regime / mission.

For the SLR-based missions the mean error over the fit-span is generally less than 500 meters, and the maximum error is generally within 1 km. This is within what would be expected in nominal operations.

For the Intelsat missions, the error is significantly larger. However, multi-kilometer error over long fit-spans at GEO is not unreasonable. This is likely due to the crude lunar perturbation modeling in the classical SGP4 algorithm; but further tuning might yield a better fit.

5.4 SGP4-XP TLE Generation

The results from the SGP4-XP TLE fit process are presented in Table 4. Note that no modifications are made to the tuning or fit-span between the classical SGP4 fit and the SGP4-XP fit, other than that SGP4-XP can estimate both B* and AGOM separately. Therefore, these results demonstrate purely the differences in accuracy resulting from the choice of propagator. Further accuracy improvements may be possible by adjusting tuning parameters.

Table 4: SGP4-XP Fit Performance (vs Classical SGP4)

	Mean Range (km)		Max Range (km)		Mean Improvement %	Max Improvement %
Mission	**SGP4**	**SGP4-XP**	**SGP4**	**SGP4-XP**		
Larets	0.552	0.548	1.277	1.221	0.8	4.4
Stella	0.528	0.511	1.155	1.108	3.2	4.1
Starlette	0.368	0.355	0.883	0.875	3.7	0.9
Lares	0.385	0.382	1.163	1.121	0.8	3.6
Ajisai	0.283	0.285	0.680	0.740	-0.9	-8.9
Lageos2	0.188	0.097	0.457	0.239	48.4	47.6
Lageos1	0.125	0.125	0.280	0.260	0.0	7.3
Etalon2	0.283	0.084	0.725	0.167	70.3	77.0
Etalon1	0.244	0.072	0.696	0.141	70.7	79.7
IS-28	1.532	0.186	3.512	0.458	87.9	87.0
IS-1R	0.905	0.082	1.455	0.214	91.0	85.3
IS-19	7.440	0.222	15.144	0.540	97.0	96.4
IS-21	7.539	0.145	13.359	0.335	98.1	97.5

The three different orbit regimes show distinct patterns. In the LEO regime, the quality of the SGP4-XP fits are generally in family with the classical SGP4 fit. This isn't too surprising, as the main disturbing perturbation is drag which is difficult to model without near real-time information about the atmospheric activity, which isn't modeled in either the SGP4 or SGP4-XP algorithms.

In the MEO regime, the quality of the SGP4-XP fits are generally much better than the classical SGP4 fit. In this orbit regime, the dynamics vary relatively slowly, so improvements in Earth potential field modeling and lunar perturbations stand to improve the quality of the propagation.

The most significant improvement comes in the GEO regime. There are likely many factors that play into this; these include the improved resonance modeling and the improved lunar perturbation modeling. At GEO, lunar perturbations tend to become a significant secondary perturbation that drives variations in the eccentricity of the orbit. Also, the more accurate modeling and use of higher-order terms associated with the tesseral perturbations from the Earth gravity field may be helping to drive the magnitude of the improvement.

5.5 Post Fit Span Propagation

The previous section details the propagation quality of the SGP4-XP versus the classical SGP4 algorithm over the fit span. While not ideal, sometimes it is necessary to use TLE's to propagate states beyond the fit span as the TLE state becomes stale. The most obvious operational scenario is when an interface with a TLE provider goes down for some period of time. Other examples might include performing coarse long term planning, general limitations in the concept of operations for a given mission, and tracking trends in the concept of operations of non-cooperative missions.

A benefit of the SGP4-XP algorithm, with its better overall modeling of physical dynamics, is a better fit of not just the position terms, but also the velocity terms. Traditionally TLE's have mainly been used in contexts where positional fits are the primary concern. However, with an improved velocity fit, it can be expected to get better post fit-span propagation; meaning a stale TLE generated using the SGP4-XP algorithm holds up better than a classical SGP4 derived TLE.

Tables 5, 6, and 7 show the propagation accuracy as compared to the high-accuracy reference ephemerides at the fit-span duration as well as when propagated 3 and 7 days past the fit-span.

Table 5: Classical SGP4 versus SGP4-XP at Fit Span

	Mean Range (km)		Max Range (km)	
Mission	**SGP4**	**SGP4-XP**	**SGP4**	**SGP4-XP**
Larets	0.553	0.549	1.296	1.236
Stella	0.529	0.512	1.143	1.111
Starlette	0.368	0.355	0.878	0.867
Lares	0.385	0.382	1.164	1.121
Ajisai	0.283	0.285	0.675	0.735
Lageos2	0.188	0.097	0.459	0.240
Lageos1	0.125	0.125	0.280	0.260
Etalon2	0.282	0.084	0.725	0.167
Etalon1	0.244	0.072	0.696	0.141
IS-28	1.530	0.186	3.513	0.459
IS-1R	0.904	0.082	1.455	0.214
IS-19	7.442	0.223	15.176	0.541
IS-21	7.540	0.145	13.360	0.336

Table 6: Classical SGP4 versus SGP4-XP at Fit Span + 3 days

	Mean Range (km)		Max Range (km)	
Mission	**SGP4**	**SGP4-XP**	**SGP4**	**SGP4-XP**
Larets	0.567	0.551	1.541	1.237
Stella	0.644	0.670	2.576	2.276
Starlette	0.464	0.471	1.455	1.416
Lares	0.422	0.397	1.282	1.121
Ajisai	0.304	0.318	0.829	0.886
Lageos2	0.214	0.098	0.515	0.247
Lageos1	0.131	0.128	0.333	0.291
Etalon2	0.416	0.098	1.181	0.242
Etalon1	0.287	0.076	0.782	0.165
IS-28	2.258	0.277	9.196	0.685
IS-1R	1.080	0.121	2.634	0.348
IS-19	8.709	0.330	19.108	0.832
IS-21	8.136	0.215	15.354	0.520

Table 7: Classical SGP4 versus SGP4-XP at Fit Span + 7 days

	Mean Range (km)		Max Range (km)	
Mission	**SGP4**	**SGP4-XP**	**SGP4**	**SGP4-XP**
Larets	0.633	0.574	1.983	1.557
Stella	1.428	1.525	6.194	5.572
Starlette	0.917	0.858	3.212	2.815
Lares	0.696	0.479	2.697	1.571
Ajisai	0.500	0.392	1.801	1.011
Lageos2	0.268	0.102	1.037	0.252
Lageos1	0.157	0.140	0.517	0.372
Etalon2	0.899	0.120	3.677	0.340
Etalon1	0.505	0.099	2.329	0.287
IS-28	4.811	0.399	19.737	1.043
IS-1R	1.844	0.175	9.444	0.565
IS-19	10.666	0.475	26.624	1.234
IS-21	9.196	0.310	19.603	0.838

There are two takeaways to pull from the data shown in these tables. The first is to recognize that for a given propagation duration, the overall behavior across orbit regimes remains similar, although the SGP4-XP propagation does hold up somewhat better. The second takeaway is that for the MEO and GEO orbit regimes the accuracy at 7 days post fit-span holds up as well as the classical SGP4. This provides some affordances for usage of stale TLE's in mission operations, for scenarios like those discussed above.

So, while the propagation performance of the SGP4-XP is shown to be generally much better in assessing the positional range between propagated states and the reference ephemeris, another benefit is the improved velocity solution. The improved velocity solution enables better post-fit propagation, and hence greater flexibility in the use of the TLE's.

5.6 Runtime Performance Analysis

A major discriminator of the classical SGP4 algorithm is that it executes a multi-day propagation very quickly and efficiently. This may be particularly relevant in legacy operational environments where the implementation of the SGP4 algorithm is applied on old and / or limited functionality systems. Of course the sacrifice is the propagation accuracy.

So, while the SGP4-XP addresses some propagation accuracy issues, particularly in the MEO and GEO regime, a potential concern with using the SGP4-XP algorithm versus the classical SGP4 is any runtime performance impacts that might be incurred.

Table 8 shows the runtime of a 7-day propagation using the classical SGP4 versus the SGP4-XP.

Table 8: SGP4 vs. SGP4-XP Runtime Performance

Mission	SGP4 Runtime (sec)	SGP4-XP Runtime (sec)	Percent Difference (%)
Larets	1.403	1.436	2.352
Stella	1.404	1.431	1.923
Starlette	1.467	1.467	0.000
Lares	1.395	1.425	2.151
Ajisai	1.413	1.486	5.166
Lageos2	0.798	0.774	-3.008
Lageos1	0.747	0.768	2.811
Etalon2	0.779	0.784	0.642
Etalon1	0.760	0.771	1.447
IS-28	0.740	0.768	3.784
IS-1R	0.755	0.773	2.384
IS-19	0.768	0.776	1.042
IS-21	0.782	0.789	0.895

The runtime performance is fairly comparable between the classical SGP4 and the SGP4-XP algorithms. It is worth noting that this is performed on a modern Windows laptop within the FreeFlyer execution environment. So while the executions times are in family with each other, in a highly optimized multiprocess / multithreaded environment for very large scale problems, these relatively small performance differences could make a significant difference. In the context of a single mission or relatively small scale constellations, the performance differences may not be significant.

It is also relevant to capture the runtime performance of the TLE fit process. This is likely less relevant given that the estimation process will likely be done on more modern hardware as part of a broader ground system that performs other much more computationally intensive operations. Additionally, there is overhead in the estimation process which could overwhelm the propagation time. However, there is also the possibility that one algorithm may exhibit better convergence behavior, hence requiring fewer iterations of the BLS process, and fewer overall propagations over the fit-span.

Table 9 shows the fit runtime for each mission using both the classical SGP4 and the SGP4-XP algorithms.

Table 9: Classical SGP4 vs. SGP4-XP Fit Runtime Performance

	Iteration Count		Runtime		
Mission	SGP4	SGP4-XP	SGP4 Fit (sec)	SGP4-XP Fit (sec)	Runtime Difference (%)
Larets	3	3	0.265	0.429	61.9
Stella	3	3	0.215	0.380	76.7
Starlette	3	3	0.227	0.402	77.1
Lares	3	3	0.265	0.394	48.7
Ajisai	3	3	0.166	0.310	86.7
Lageos2	3	3	0.469	0.839	78.9
Lageos1	3	3	0.500	0.819	63.8
Etalon2	3	3	0.068	0.191	180.9
Etalon1	3	3	0.069	0.115	66.7
IS-28	3	3	0.039	0.109	179.5
IS-1R	3	3	0.039	0.108	176.9
IS-19	11	3	0.142	0.112	-21.1
IS-21	3	3	0.041	0.105	156.1

This shows that the fit process using SGP4-XP takes a little less than twice the runtime as the classical SGP4 given the same number of iterations. In this process the same convergence criterion is used for all missions. The convergence criterion is evaluated as the percent change in the overall weighted root-mean-square (WRMS) between iterations. When that metric meets 1.0%, convergence is met.

It is worth noting the convergence behavior using the classical SGP4 for IS-19 in Table 9 is out of family with the other missions. This is an indicator that the more coarse lunar perturbation and resonance models in the classical SGP4 aren't fully capturing the dynamics for that particular case.

6. EXAMPLE PROBLEMS

With the analyses outlined above, example scenarios where the SGP4-XP algorithm can act as a discriminator are evaluated. Since the SGP4-XP provides the biggest gains over classical SGP4 in the GEO orbit regime, the example problems will focus on GEO scenarios. The example problems (a contact analysis problem and a conjunction assessment problem) will focus on the differences in the quality and usefulness of the results when using the SGP4-XP algorithm as compared to the classical SGP4 algorithm.

For both examples a notional error of 5 km is applied relative to a defined truth for evaluation for the classical SGP4 algorithm, and a notional error of 500 m for SGP4-XP algorithm. This relative difference is generally consistent when evaluating the error between the high-fidelity propagation versus that of the SGP4 propagation at about halfway through the fit-span. The manner in which the error is applied varies between the two examples problems and will be discussed in those sections.

Note that these problems are only intended to provide a rough idea and visual concept of the impact of the errors associated with one algorithm versus another. The errors associated with both SGP4 algorithms with respect to high-fidelity models are not Gaussian, and hence no probabilistic analysis is considered in this context. With that in mind the general approach is to present the envelopes of expected behavior of the various metrics of the problem based on the error level that might be in the propagated state. While the discussion generally associates the 5 km error with the classical SGP4 algorithm and the 500 m error with the SGP4-XP algorithm, it is quite possible that a given classical SGP4 propagation may have less (or more) error than the 5 km nominal value; and likewise it is possible that the SGP4-XP propagation has more error than the 500 m nominal value.

As an aside, the covariance from the fit process for each algorithm is an output that can be considered. This provides an opportunity to perform additional analysis from a probabilistic perspective using Monte Carlo or other techniques, but that is outside the scope of this paper.

Contact Analysis

The first example problem examines a low-inclination GEO mission with a very small field-of-view (FOV) sensor pointing nearly nadir towards a ground station in the continental United States. In this example, the location of the center of the sensor FOV with ideal pointing is shown as the ground site location along with the center of the FOV for each state that is misaligned given the errors in the states coming from the classical SGP4 and SGP4-XP algorithms.

This specific example problem evaluates a scenario where a GEO mission is stationed over the central continental United States and is attempting to downlink to a ground station in Maryland.

A truth orbit is defined with a low inclination. The ideal pointing angles from the sensor on the spacecraft are determined using the truth state. The impact of different error levels is assessed in determining the strike point of the boresight of the sensor relative to ideal given the error in the pointing angles coming from the error in the state. In this analysis the errors are applied in the alongtrack and crosstrack directions of the orbit. This 2D projection of the error is used since the radial error would have near-zero impact for this example problem.

Figure 3a shows a static analysis of the potential strike point of the boresight given different error levels in the state. In this visualization, the ground site at NASA GSFC is the target for the downlink. With ideal pointing, i.e. no error in the spacecraft state, the boresight would target the NASA GSFC ground site directly. The contours in Figure 3a provide an indication of where the boresight might strike the Earth surface when different error levels are applied to the state. Again, there is no particular distribution to the error in this example problem, but the visualization provides an envelope of what might be expected given the error associated with a given algorithm.

The thick red line in Figure 3b represents the envelope in which the ground site will scan to develop a lock and acquisition of signal. As the strike point of a misaligned sensor gets nearer the edge of the ground site's scan area, acquisition and signal lock becomes more difficult.

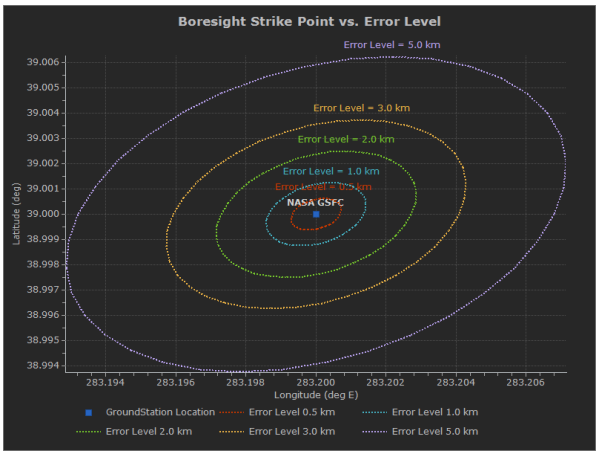

(a) Pointing Errors Envelopes for Different State Errors

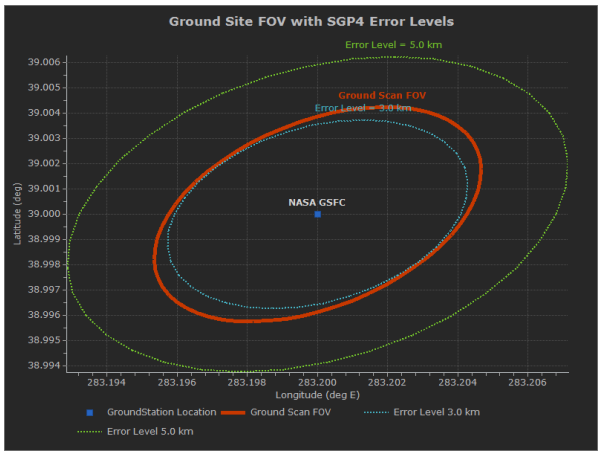

(b) Ground Site Field of View with SGP4 Error Levels

Fig. 3: State Error Impact on Pointing

As can be seen in this visualization, when applying error levels associated with the SGP4 algorithm, the boresight strike location may be outside the ground site's scan area when using pointing based on a state with no error. However, when using error levels associated with the SGP4-XP algorithm, it is reasonable to expect that obtaining acquisition and lock may be significantly easier.

While this doesn't represent a rigorous analysis, it provides some insight into how the state errors from the different algorithms maps into the realm of satellite to ground site communications.

Conjunction Assessment (CA)

The second example problem examines two GEO missions with a similar longitude of equator crossings. In this example, the effect of the error from both the classical SGP4 and the SGP4-XP on conjunction metrics is characterized.

While it is generally poor practice to use TLE's for advanced conjunction assessment, it can be useful to perform a coarse evaluation of a scenario or trends in scenarios. It is critical, however, to have in mind the level of accuracy / error that might be in the data under evaluation.

This example problem evaluates two missions stationed at a very similar longitude of equator crossing. One mission holds a low inclination of about 0.1 degrees, while the other is allowed to drift at around 5 degrees of inclination. In this scenario, there are possible conjunctions at the equator crossing every 12 hours or so.

The analysis approach defines a truth orbit for both missions where the problem is designed to have the truth trajectories intersect at the node crossing. The scenario starts by applying state errors to the mission with the higher inclination 6 hours prior to the node crossing. As is done in the previous problem, multiple error levels are evaluated to determine the envelope of possible conjunction metrics, rather than trying to do any probabilistic analysis. Unlike the previous problem, the error is applied in the 3 components of alongtrack, crosstrack and radial separation. From this, each error state is propagated to the node crossing, then their individual time-of-closest approach (TCA) with the low-inclination mission is calculated.

Figure 4 shows metrics from the conjunction data from all error states sampled. All the metrics are evaluated at TCA. The metrics chosen are absolute range difference (miss-distance) and radial difference at TCA between the truth states and the error states.

These metrics are presented in a similar manner as is done for the first example. The envelope of the expected ranges of each metric based on state possible error level is presented. As mentioned above, it is assumed that the classical SGP4 algorithm has an error level of approximately 5 km, while the SGP4-XP algorithm is more in the 500 m range. However, particularly in the context of conjunction assessment it is very important to have an understanding of the error in the states that are being evaluated.

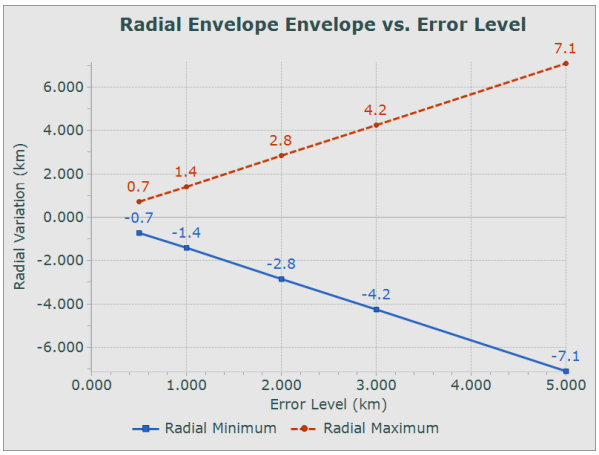

(a) Minimum and Maximum Radial Separation at TCA vs. Error Level

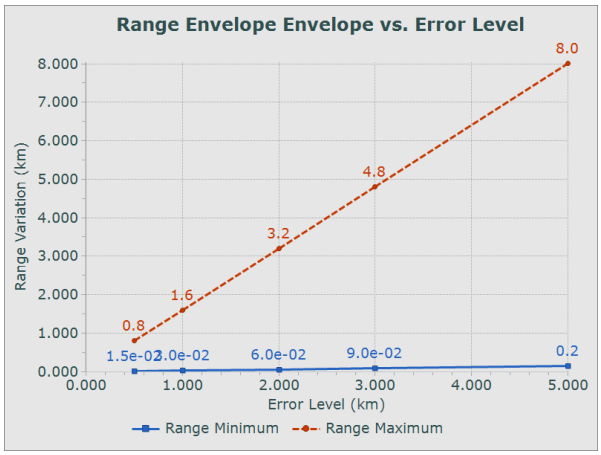

(b) Minimum and Maximum Range at TCA vs. Error Level

Fig. 4: Metrics for Example GEO CA Problem

In the absence of covariance and the ability to perform probabilistic analysis, the key metrics usually evaluated are overall miss distance and radial separation at TCA.

Figure 4a shows the envelopes of the miss-distance in the radial direction. This constitutes most of the overall miss-distance. The radial separation is also a key metric used in evaluating the magnitude of ΔV required to mitigate a conjunction. Again, formal maneuver planning should only be done with high-fidelity data, but a rough feel on the impact to operations might be discernible if the amount of error in the state is considered. In this example, the ΔV to achieve a $\pm$ 7 km radial separation would need to be considered. This is probably not practical from an operational perspective. When using an error level more consistent with the SGP4-XP algorithm, some information can still be resolved; specifically, the worse case ΔV that is required as well as some potential insight into the conjunction geometry.

The main takeaway from Figure 4b is that when using the classical SGP4 algorithm the overall miss distance can be off be as much as 8 km or more, whereas when using the SGP4-XP it isn't unreasonable to expect miss distances to be less than 1 km. This magnitude difference is particularly significant in that it could drive whether events are flagged based on control volume sizes. It is fairly common practice to use a coarse filter on miss distance in various components to signify that an event warrants higher fidelity analysis. Given an operational approach that uses a 5 km control volume, a propagated state with 8 km of error could lead to a missed event. In summary, the best information that be obtained when using the classical SGP4 algorithm for CA analysis for this sort of problem is trending information for the identification and possibly prediction of future events. However, even in that scenario the error in the states may be significant enough that events are missed altogether (or false events may be detected).

When using the SGP4-XP algorithm for CA analysis for this sort of problem, the data is accurate enough to provide some feel for conjunction geometry, severity, impact to mitigate, and greater confidence in the trending of events.

7. OBSERVATIONS, CONCLUSIONS, AND FUTURE WORK

Overall, the SGP4-XP algorithm exhibits behavior that reflects better overall physical modeling. Even in the LEO regime, where the fit quality over the fit-span is comparable to the SGP4 algorithm, the better modeling provides a more realistic profile of the velocity and hence a significantly better post-fit span performance.

The improved resonance modeling is particularly apparent in the MEO and GEO orbit regimes where the fit-span accuracy is generally almost an order of magnitude better. And as is the case for the LEO orbit regime, post-fit propagation holds up well and mostly stays well within the accuracy of the classical SGP4 even 7 days post fit.

The execution time of the SGP4-XP is generally longer than that of the classical SGP4, but not significantly so. Also, it is worth noting that convergence behavior of the SGP4-XP fit process is generally better than the classical SGP4

fit. This is expected given that the SGP4-XP algorithm more accurately reflects the true dynamics of the orbit. This behavior means that even though the raw propagation time may be longer using the SGP4-XP algorithm, the state estimation process as a whole may be in family as that when using the classical SGP4 depending on the convergence criteria.

In performing this analysis, it was seen that at times the B^* term and the AGOM term could alias each other in the fit. As both terms represent non-conservative forces, sometimes in a loosely tuned fit process those terms can absorb unmodeled dynamics that aren't strictly related to the drag and / or SRP accelerations. Between iterations of the BLS, those unmodeled dynamical errors can be accounted for in B^* term for one iteration, then the AGOM term for the next. This can lead to thrashing in the BLS fit process. Some basic tuning, based on orbit regime, seemed to remedy this issue easily.

It is worth noting that in general this analysis was done while providing as little tuning as possible. The concept is to present the "out-of-the-box" behavior for the two algorithms. The metrics presented in this paper are not intended to demonstrate the best performance possible, but rather the general behavior available. More advanced tuning analysis may lead to better performance, particularly in the LEO orbit regime.

Another area of future work is to use the approach outlined in this paper to perform covariance analysis. As noted above, the fit process used here provides a covariance in the mean equinoctial frame. Monte Carlo and other techniques may provide the ability to do probabilistic analysis rather than using the envelopes presented in the example problems, which what amounts to a white-noise distribution. Intuition suggests that the more realistic dynamics coming from the SGP4-XP algorithm yields a structure in the error which is more Gaussian than that of the classical SGP4.

For all the benefits that the SGP4-XP provides it is imperative to note that an SGP4-XP state is **not** compatible with the classical SGP4 propagator. In other words, a state that is derived using the SGP4-XP algorithm must be propagated with the same algorithm of the SGP4-XP propagator that was used to do the fit. For example, if a new mission is using FreeFlyer to generate a TLE it might be tempting to always generate the TLE using the SGP4-XP algorithm. However, it is critical that all users (such as ground sites) of those TLE's then use the same SGP4-XP algorithm when propagating TLE states.

ACKNOWLEDGEMENTS

Thank you to Sara Fields, and the rest of the FreeFlyer product team in supporting this analysis, providing advice in the performing the analysis described above, and helping in the review process.

REFERENCES

[1] F. R. Hoots and R. L. Roehrich. Spacetrack Report #3: Models for propagation of the NORAD element sets. Technical report, U.S. Air Force Aerospace Defense Command, Colorado Springs, CO, December 1980.

[2] D. A. Vallado, P. Crawford, R. Hujsak, and T. S. Kelso. Revisiting Spacetrack Report #3. In *AIAA/AAS Astrodynamics Specialist Conference*, Keystone, CO, 2006. American Institute of Aeronautics and Astronautics.

[3] F. R. Hoots, P.W. Jr. Schumacher, and R. A. Glover. History of analytical orbit modeling in the U.S. Space Surveillance System. *Journal of Guidance, Control, and Dynamics*, 27(2):174–185, 2004.

[4] HQ Space Operations Command (SpOC) DCG-T/S9I Astrodynamics Standards Engineering Group. Astrodynamics Standards release notes version 8.3. Technical report, April 2022.

[5] D. A. Vallado and P. J. Cefola. Two-line element sets – practice and use. In *63rd International Astronautical Congress*, Naples, Italy, 2012. International Astronautical Federation.

[6] T. S. Kelso. Validation of SGP4 and IS-GPS-200D against GPS precision ephemerides. In *17th AAS/AIAA Space Flight Mechanics Conference*, Sedona, AZ, 2007. American Astronautical Society.

[7] 2022.

[8] David A Vallado. Covariance transformations for satellite flight dynamics operations. 2004.